Journal Name

RSCPublishing

ARTICLE

An electrochemical analyzer for *in situ* flow determinations of Pb(II) and Cd(II) in lake water with on-line data transmission and a global positing system

Cite this: DOI: 10.1039/C4AY01811G

Received 31 Jul 2014,

Accepted 27 Aug 2014

www.rsc.org/

Vagner Bezerra dos Santos[a,*], Elson Luiz Fava[a], Newton Sá de Miranda Curi[b], Ronaldo Censi Faria[a], Thiago Brito Guerreiro[a] and Orlando Fatibello-Filho[a]

Electronic Supplementary Information (ESI)

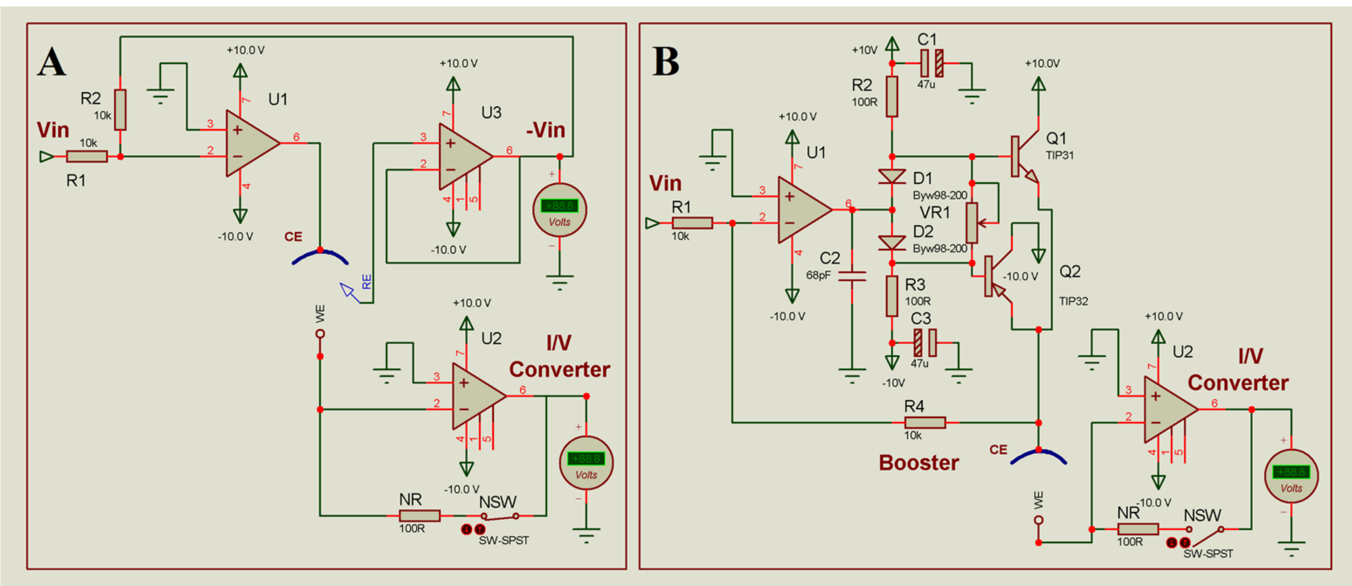

Fig. S1. Basic electronic circuits of the potentiostat (A) and galvanostat (B). In the galvanostat, the RE was not used and a current booster was developed. The Vin, −Vin, and I/V are the applied potential, inverted potential, and current-to-potential converter, respectively. The virtual ground manifold was employed in the WE. NR represents the possibility of up to seven resistors that can be selected by each one of the seven switches (NSW) used to set the desired current range in the potentiostat or galvanostat mode.

As presented in Fig. S1 (A), the inverter manifold was employed in the operational amplified (U1). The inverted initial potential difference (−Vin) is supplied in the CE, and subsequently, in the electrochemical cell. The WE is kept in virtual ground at U2, and high impedance (1.0 TΩ) in the RE is ensured due to input of U3. Two 12 V batteries in series were used as power supply, and a voltage regulator was employed to supply ±10 V. The potential difference is measured at outlet from U3 and U2 and the current is measured by the current-to-voltage converter (I/V) configured in U2. The electronic circuit of the galvanostat is similar to the potentiostat (Fig. S1 B), expect by the absent of the RE. Moreover, in this electronic circuit, a booster current was developed to supply a high electric current in the galvanostat.

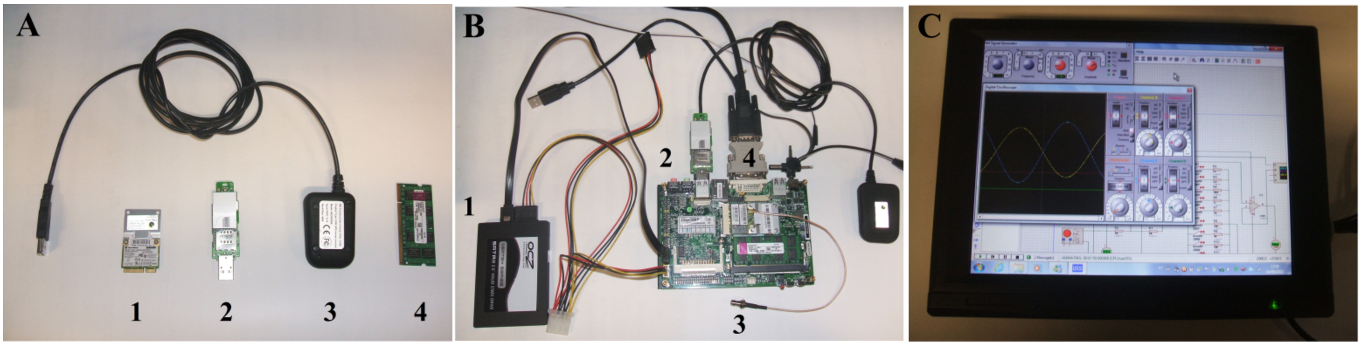

Fig. S2. Peripherals coupled to the CPU from the PG0004. In A, 1: Bluetooth and Wi-Fi wireless board, 2: 3G modem for GPRS communication, 3: GPS receiver, and 4: RAM memory. In B are shown the peripherals in A that were connected to the CPU, and 1: HD, 2: CPU, 3: wireless antenna, 4: VGA output for touchscreen monitor presented in C.

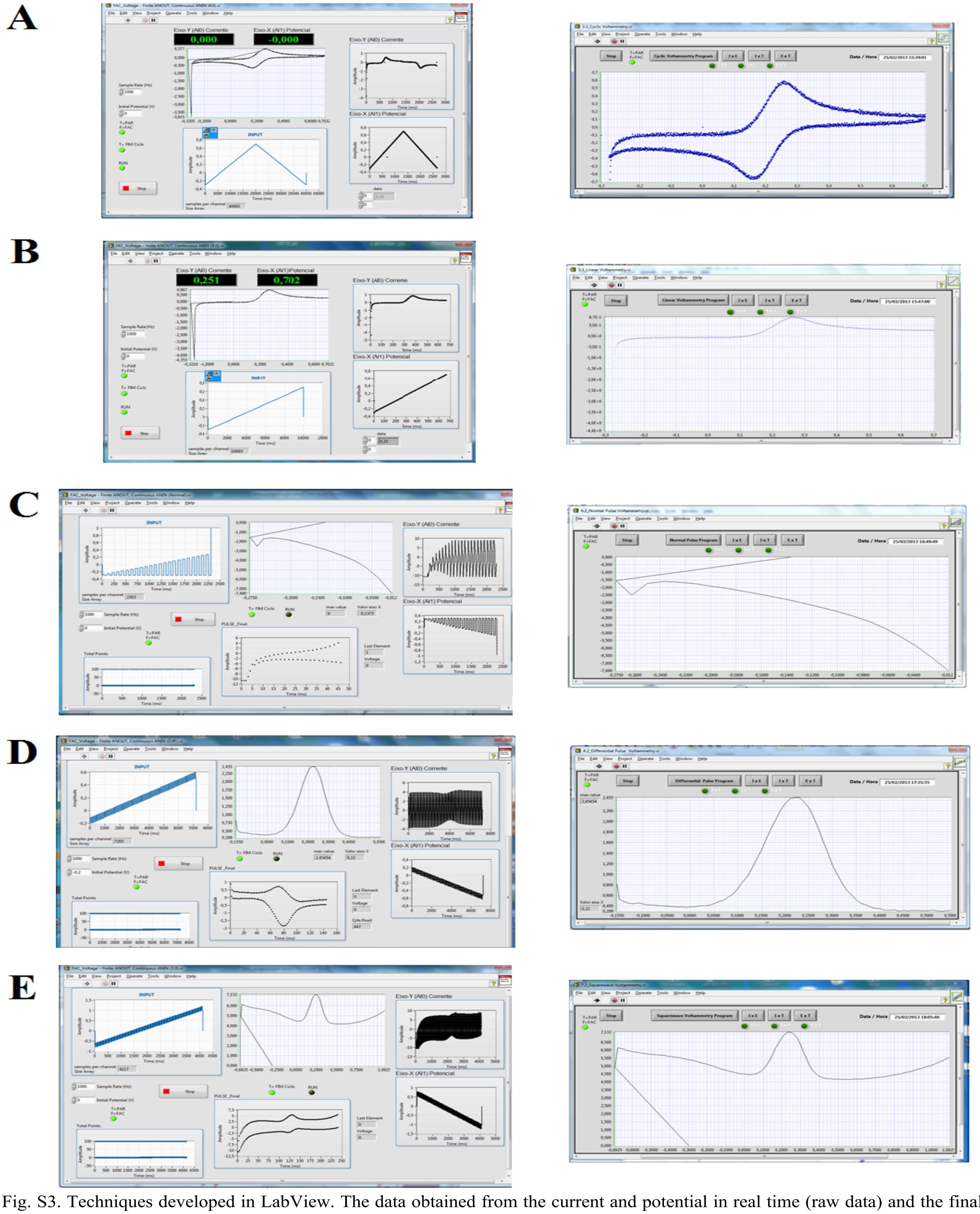

Fig. S3. Techniques developed in LabView. The data obtained from the current and potential in real time (raw data) and the final results of the experiments. Voltammetry: cyclic (A), linear (B), normal pulse (C), differential pulse (D), and square wave (E) are shown. Parameters employed for CV and LV – sweep potential: -0.3 V to 0.7 V, and υ: 50 mV s^{-1}. Parameters employed for NPV – ΔE: 25 mV, a: 50 mV, and ΔT: 100 ms. Parameters employed for DPV – ΔE: 10 mV, ΔT: 100 ms, t: 50 ms, and a: 90 mV. Parameters employed for SWV – ΔE: 5 mV, f: 30 Hz, a: 100 mV. Scale current: 100 µA.

RSCPublishing

ARTICLE

As presented in Fig. S3 (A), the cyclic voltammetry (CV) technique was well characterized by application of a staircase potential in which small increments of potential (mV) were applied per time unit (s), e.g. mV s^{-1}, generating the sweep rate (υ). Similarly, the linear voltammetry (LV) technique can be observed (Fig. S3 B).

In normal pulse voltammetry (NPV); Fig. S3 (C), pulses of potential were continuously applied until the *n* pulse reached the value of potential established in the potential window chosen. Pulses in NPV were characterized by their return to baseline potential, with υ given by ΔE (mV) / ΔT (ms), where ΔE is the potential increment and ΔT is the time interval between the pulses (step time). Overall, ΔT was always longer than the pulse duration (t), as is required. The current signal obtained at the end of the pulse was subtracted from that obtained at the beginning of the pulse.

The technique of differential pulse voltammetry (DPV), Fig. S3 (D) also presented some parameters used in the NPV technique; however, the applied potential pulses consisted of pulse amplitude (a) plus ΔE. Afterwards, when the pulse is returned, only the amplitude is applied, creating a kind of staircase, wherein each step of this is increased by the applied ΔE. The resulting current signal was obtained by subtracting the current measured at the end of each pulse by the current measured immediately at the beginning of the pulse.

The square-wave voltammetry (SWV) consisted of potential pulses that were applied symmetrically with respect to a potential baseline with an increment given by ΔE. Thus, current signals were generated due to the contribution of the forward and backward potentials, as shown in Fig. S3 (E). In this case, $\upsilon = \Delta E$ (mV) $\times$ f (Hz), with f (Hz) = 1 / T (s), and T (s) = 2 $\times$ t.

As can be seen in Fig. S4, for all voltammetric methods, the programmable potential applied waveform (in blue) was electronically inverted and applied in the electrochemical cell (in yellow), and it was correlated with the electric current that was converted to potential by an I/V converter in the PG, generating the yellow waves in Fig. S4. The current needs to be treated according to the criteria of each technique to be presented in a conventional format (Fig. S3). Thus, the CV, LV, NPV, DPV, and SWV are shown in Fig. S4. Moreover, the straight lines parallel to the x-axis (time) presented in all electrochemical methods refer to the standby potential setup, i.e., 0.0 V.

ARTICLE

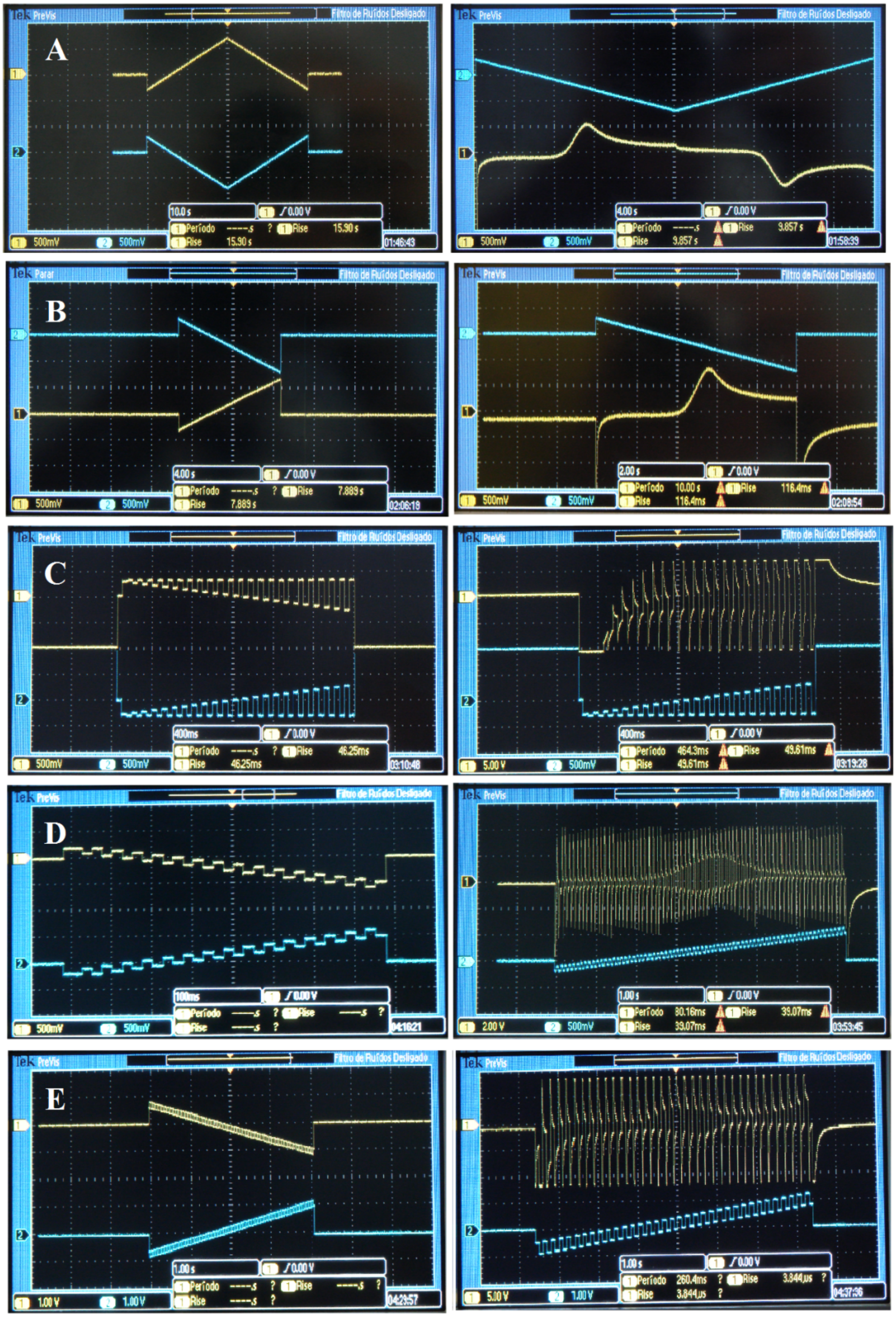

Fig. S4. Tests performed using the PAR model 173A and the oscilloscope employing the developed software. Applied potential (blue curves) and the potential available in the electrochemical cell (yellow curves), and the generated current (yellow curves) are shown. From A to E are presented the voltammograms from: cyclic, linear, normal pulse, differential pulse, and square wave.

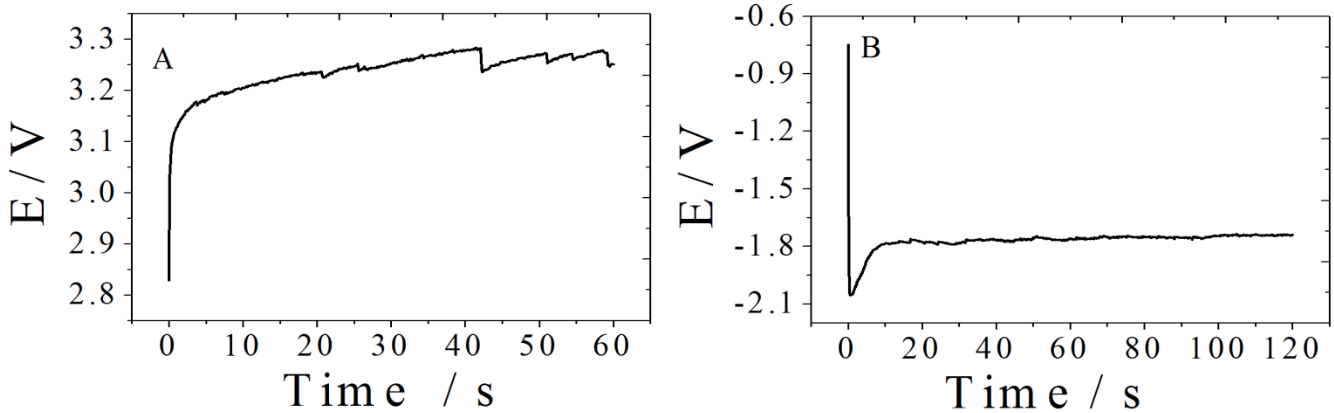

Fig. S5. Chronopotentiometric curves applied in the anodic (A) and cathodic pre-treatments (B) of the BDD electrode using the PG004. In (A) 50 mA cm^{-2} was applied for 60 s, and (B) –50 mA cm^{-2} for 120 s in 0.1 mol L^{-1} H_2SO_4 as supporting electrolyte.

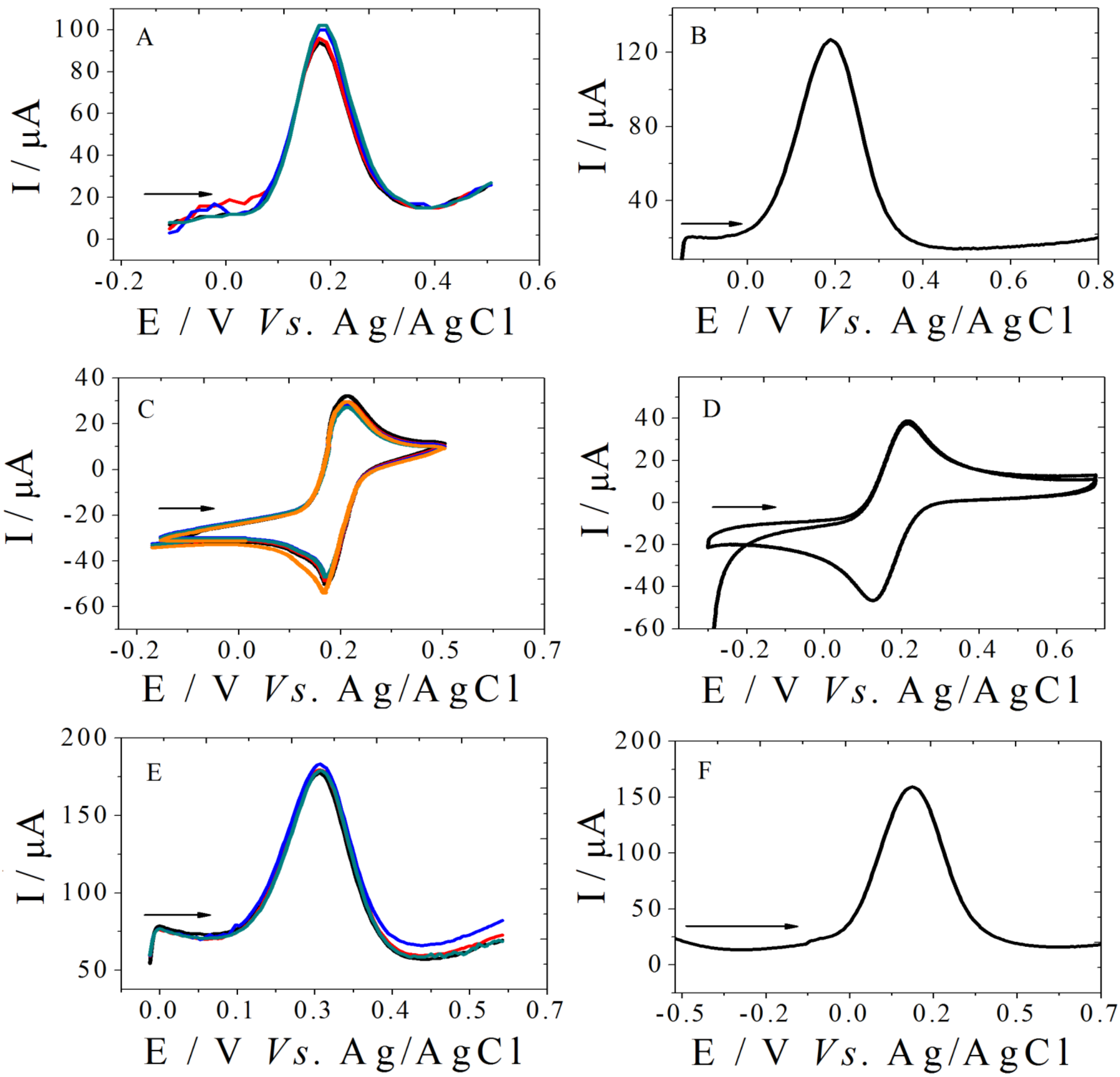

Fig. S6. Voltammetric determinations carried out using the PG004 and PG581. In (A), (C), and (E), the DPV, CV, and SWV waves obtained using the PG004 are shown. In (B), (D), and (F), the respective voltammograms employing the PG581 are shown. The voltammograms were obtained using the SPE-BDD in 1.0×10^{-3} mol L^{-1} of potassium hexacyanoferrate (III) solution in 1.0 mol L^{-1} KCl. For CV and LV, a sweep rate of 50 mV s^{-1} was employed. For DPV – increment: 25 mV, pulse height: 50 mV, step time: 100 ms. For DPV – increment: 10 mV, step time 100 ms, pulse width: 50 ms, pulse height: 90 mV. For SWV – increment: 5 mV, frequency: 30 Hz, pulse height: 100 mV.

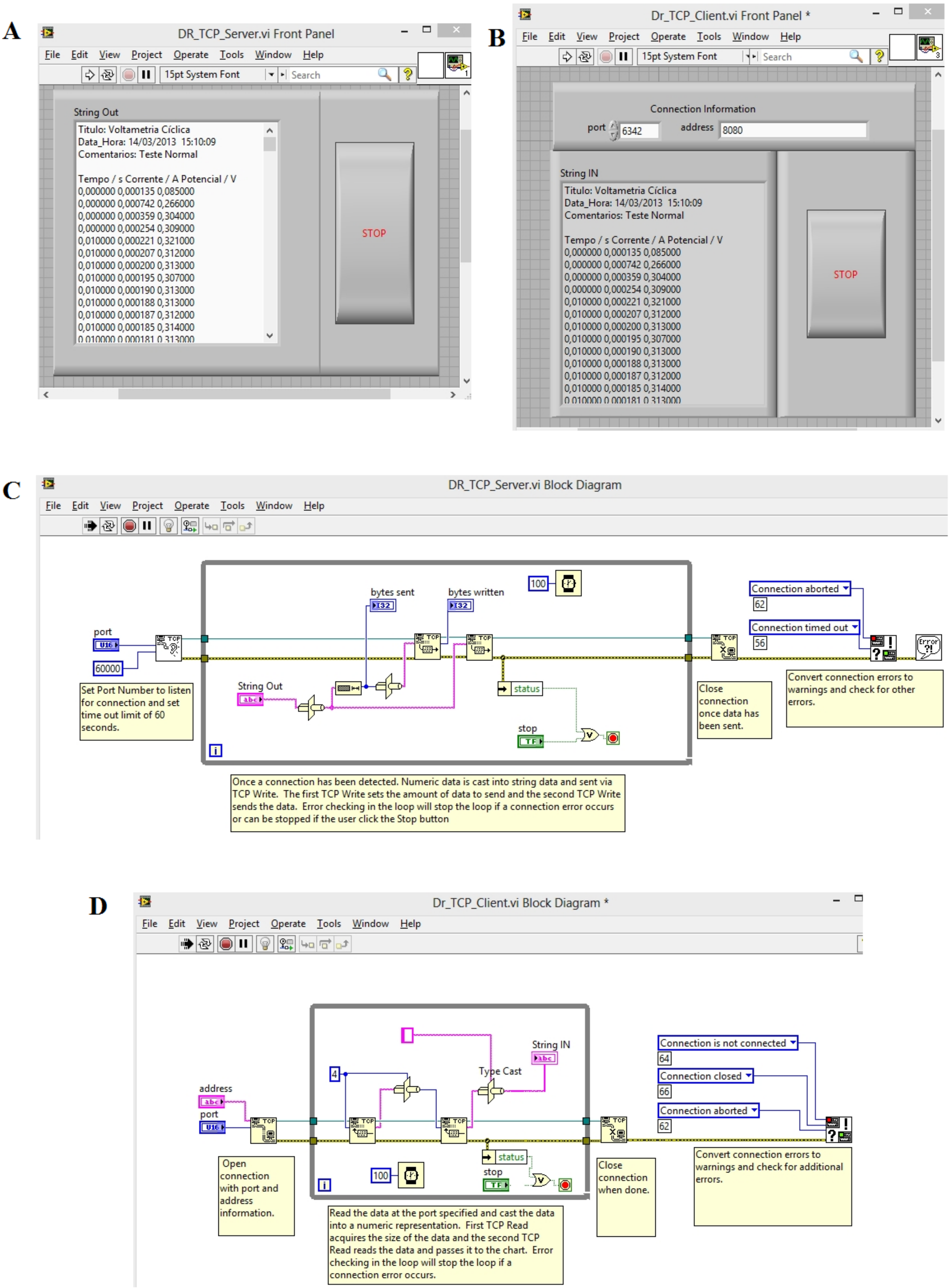

Fig. S7. Transmission communication protocol for the internet protocol (TCP/ IP) using a Wi-Fi network and the server system (A and C) and client (B and D) developed in LabView software, which was used to send cyclic voltammetry data.

Fig. S8. *In situ* analysis using the PG004. (A) Dam of Monjolinho Lake, (B) a photograph of PG004, and extra batteries (C) being recharged employing the solar boards. In (D), the sample being collected and in-line filtered (indicated by the arrow) using a 0.45 μm filter is shown. The real temperature of the sample onto the EFC by using the thermostated control driven by the microcontrolled board developed (E). Waste bottle (F).

A

B

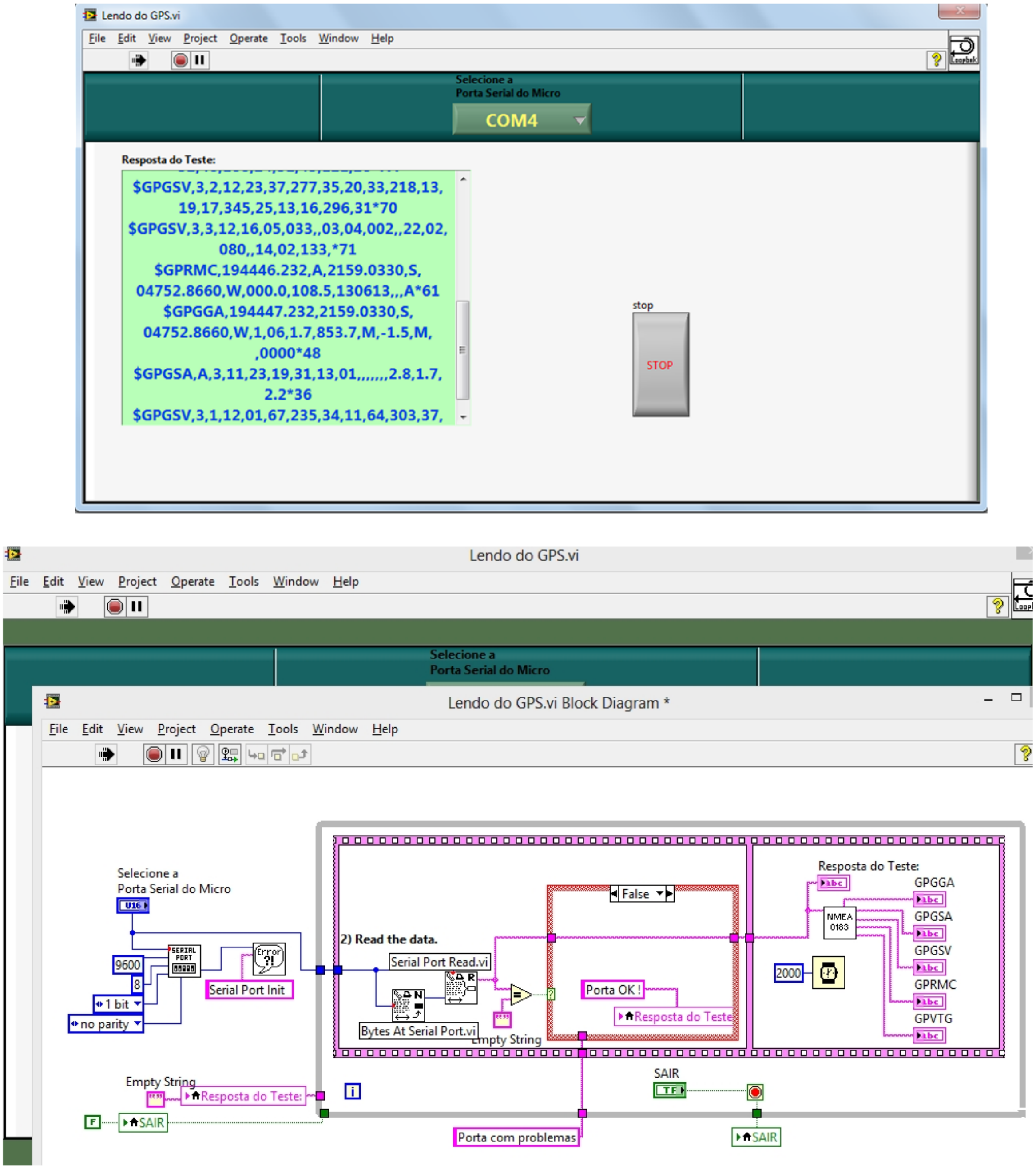

Fig. S9. Receiving data via GPS. Data in the NMEA navigation protocol using the COM4 serial port from the CPU of the PG004 (A). Block diagram of the program developed in LabView (B).

Each sentence starts with symbol "$" and the letter "G" features of the GPS receiver and ends with the symbol "*" followed by a checksum that evaluates the conformity of transmission. Each sentence presents distinct information, but may contain some similar data. For the ME2000RW receiver, the main sentences (GPGSA, GPGGA, and GPRMC) are further highlighted. For the GPGSA, it is possible to identify what type of information is being sent by the satellites, for example, in the sentence: $ GPGSA, **A**, **3**,11,23,31,13,01,20,32, , , , , ,2.8,1.6, 2.3 * 3D, the code "**A**" means "automated", i.e., automated data, and code "**3**" refers to 3D data, i.e., latitude, longitude, and altitude. For the GPGGA code, information about fixed data are supplied, as in this sentence: $ GPGGA, **200558**.234,**2159.1203, S**, **04752.9038, W**, 1,**07**,1.6,**803.1**, M,-1.5, M, 0000*46. The highlighted codes "**200558**", "**2159.1203**, S", "**04752.9038**, W", "**07**", and "**803.1**, M" refer to the precise time (**20:05:58**), the latitude (**21°59.1203'S**), and the longitude (**47°52.9038'W**) provided by seven synchronized satellites (**07**), and altitude in feet (**803.1**), respectively. This time is based on the universal time coordinated (UTC), i.e., as São Carlos-SP, Brazil is 3 h behind of this time zone, the local time was 17:05:58. GPRMC describes the recommended minimum data to send, e.g.: $ GPRMC, **200559**,234, **A**, **2159.1203, S, 04752.9038, W,** 000.0,023.4,**130613**, , , A* 6B.

The highlighted codes refer to the time in UTC ("**200559**"), confirmation of the activation of satellite ("**A**"), the coordinates (**2159.1203, S, 04752.9038, W**), and then the date on which the data were transmitted (**13.06.13**).

